Table II. NMRD Parameters Obtained from the Fitting[a] of NMRD Profiles with the Inner- and Outer-Sphere Relaxation Theory

	DOTA	3a	3b	3c	3d
τ_{S0}, ps	460 ± 20	417 ± 18	275 ± 14	443 ± 20	300 ± 13
τ_V, ps	26 ± 8	20 ± 6	21 ± 6	14 ± 4	22 ± 6
τ_R, ps	72 ± 1	86 ± 1	115 ± 2	115 ± 2	133 ± 2
r, Å	3.16 ± 0.01	3.06 ± 0.01	3.09 ± 0.01	3.07 ± 0.01	3.03 ± 0.01

[a] The standard deviation for the calculated relaxivity is less than 0.01 in all data.

An outer-sphere contribution to the relaxation rate[25,26] was also taken into account in the fitting procedure, using a value of 3.6 Å for the distance of closest approach of Gd^{3+} complex and water molecule (a) and a value of 2.6×10^{-5} cm^2 s^{-1} for their relative diffusion constant (D). The fitting parameters are reported in Table II.

The $1/T_1$ NMRD profiles (Figures 2 and 3) of **3a–d** are consistent with the presence of one water molecule in the inner coordination sphere. The results indicate that the Gd^{3+} complexes of macrocyclic ligands **2a–d** have significantly higher relaxivities than $Gd(DOTA)^-$ over the entire magnetic field range investigated (0.01–50 MHz). The differences in relaxivity among the five Gd^{3+} chelates are due to their different values of τ_R and τ_{S0} (Table II). At high fields (>5 MHz), the relaxivities depend entirely on τ_R, which is proportional to the size and the molecular weight of the complexes, while at lower fields the contribution of τ_{S0} also becomes important. The effect of the latter parameter is particularly evident when the relaxivity profiles of the isomeric complexes **3b** and **3c** are compared with each other (Figure 3). In this case, the low-field differences in their inner- and outer-sphere relaxivities are completely accounted for by the different electronic relaxation times of the two complexes. The value of τ_{S0} seems to reflect the changes in symmetry introduced in the coordination sphere of the Gd^{3+} ion by the insertion of one, two, or three β-benzyloxy-α-propionate residues. In fact, τ_{S0} of the monosubstituted (Gd–**2a**) complex (417 ps) is lower than that of the highly symmetric $Gd(DOTA)^-$ complex (460 ps). Moreover, the difference in τ_{S0} between Gd^{3+} complexes of disubstituted ligands **2b** (275 ps) and **2c** (443 ps) is particularly impressive and may result from the lower symmetry of the 1,4-disubstituted isomer. The value of τ_{S0} depends not only on the change introduced in the molecular geometry but also on the nature of the substituent group. In fact, as reported by Sherry et al.,[7] the amidation of a DOTA carboxyl group produces a dramatic decrease in τ_{S0}, which results in a lower water proton relaxivity at low fields. Nevertheless, it must be pointed out that to ascribe the changes in τ_{S0} entirely to geometric changes represents an approximation. The electronic relaxation time at zero field, τ_{S0}, is related to τ_V through the equation[27]

$$\tau_{S0} = (12\Delta^2\tau_V)^{-1} \qquad (9)$$

where Δ^2, the quadratic zero-field splitting, is the parameter which is sensitive to the symmetry and the electronic structure of the metal ion. From eq 9 it is evident that the variation in τ_{S0} among the complexes could well arise in part from variation in τ_V. However, even though the changes in τ_{S0} have not a simple and obvious relationship to geometric changes and the product $\tau_{S0}\tau_V$ only shows a slight increase from **3b** to **3d**, we do not believe that the changes in the τ_V values reported in Table II for the five Gd^{3+} complexes have a real physical meaning, since the fitting results are quite insensitive to the actual value of this parameter. In fact, very similar τ_V values have been reported for a variety of Gd^{3+} complexes with ligands of different sizes and structures (HEDTA, EDTA, DTPA, aquo ion, etc.[14,28]). If this is true, the results of this work support the view that both τ_R and τ_{S0} may be conveniently modulated by introducing suitable substituents in the DOTA basic structure. The concomitant occurrence of long τ_R and τ_{S0} makes **3a,d** candidate contrast agents which would be particularly useful for applications at low magnetic field strength.

Registry No. **1a**·3HCl, 124628-31-5; **1b**, 124627-96-9; **1c**, 124627-98-1; **1d**·HCl, 138666-91-8; **2a**, 124628-08-6; **2b**, 124628-02-0; **2c**, 124628-04-2; **2d**, 124628-06-4; BzlClPA, potassium salt, 138666-92-9; TAZA, 294-90-6; sodium bromoacetate, 1068-52-6.

(25) Bennet, H. F.; Brown, R. D., III; Koenig, S. H.; Swartz, H. M. *Magn. Reson. Med.* **1987**, *4*, 93.
(26) Gillis, P.; Koenig, S. H. *Magn. Reson. Med.* **1987**, *5*, 327.
(27) Rubinstein, M.; Baram, A.; Luz, Z. *Mol. Phys.* **1971**, *20*, 67.
(28) Hernandez, G.; Brittain, H. G.; Tweedle, M. F.; Bryant, R. G. *Inorg. Chem.* **1990**, *29*, 985.

Contribution from the Department of Chemistry, Clemson University, Clemson, South Carolina 29634-1905

Synthesis and Structure of Infinite-Chain Copper(II) Polymer Systems

Larry W. Morgan, Kevin V. Goodwin, William T. Pennington,* and John D. Petersen*

Received July 2, 1991

Introduction

Polymeric copper complexes are of interest for their magnetic and electronic properties[1–5] and have served as model systems for biological studies.[3,6,7] Structural studies have revealed that many of these polymers involve molecular units bound together by longer-range interactions,[2–4,8,9] while relatively few others are bound by stronger, molecular interactions.[5,10–12]

Of the latter category, two compounds involve bridging pyrazine ligands to form one-dimensional chains[11] or two-dimensional sheets.[5] Hatfield and co-workers[1,15–17] have shown that the ori-

(1) Eckberg, R. P.; Hatfield, W. E. *J. Chem. Soc., Dalton Trans.* **1975**, 616.
(2) Phelps, D. W.; Losee, D. B.; Hatfield, W. E.; Hodgson, D. J. *Inorg. Chem* . **1976**, *15*, 3147.
(3) Brown, D. B.; Hall, J. W.; Helis, H. M.; Walton, E. G.; Hodgson, D. J.; Hatfield, W. E. *Inorg. Chem.* **1977**, *16*, 2675.
(4) Julve, M.; De Munno, G.; Bruno, G.; Verdaguer, M. *Inorg. Chem.* **1988**, *27*, 3160.
(5) Darriet, J.; Haddad, M. S.; Duesler, E. N.; Hendrickson, D. N. *Inorg. Chem.* **1979**, *18*, 2679.
(6) Petty, R. H.; Welch, B. R.; Wilson, L. J.; Bottomley, L. A.; Kadish, K. M. *J. Am. Chem. Soc.* **1980**, *102*, 611.
(7) Dapporto, P.; De Munno, G.; Sega, A.; Mealli, C. *Inorg. Chim. Acta* **1984**, *83*, 171.
(8) Sekizaki, M. *Acta Crystallogr.* **1973**, *B29*, 327.
(9) Willett, R. D. *Acta Crystallogr.* **1990**, *C46*, 565.
(10) De Munno, G.; Bruno, G. *Acta Crystallogr.* **1984**, *C40*, 2030.
(11) Santro, A.; Mighell, A. D.; Reimann, C. W. *Acta Crystallogr.* **1970**, *B26*, 979.
(12) Cantarero, A.; Amigo, J. M.; Faus, J.; Julve, M.; Debaerdemaeker, T. *J. Chem. Soc., Dalton Trans.* **1988**, 2033.
(13) Brewer, G.; Sinn, E. *Inorg. Chem.* **1985**, *24*, 4580.
(14) Real, A.; Zarembowitch, J.; Kahn, O.; Solans, X. *Inorg. Chem.* **1987**, *26*, 2939.
(15) Richardson, H. W.; Hatfield, W. E. *J. Am. Chem. Soc.* **1976**, *98*, 835.
(16) Richardson, H. W.; Wasson, J. R.; Hatfield, W. E. *Inorg. Chem.* **1977**, *16*, 484.
(17) Blake, A. B.; Hatfield, W. E. *J. Chem. Soc., Dalton Trans.* **1978**, 868.

0020-1669/92/1331-1103$03.00/0

Table I. Crystal Data

emp formula:	$C_8H_{12}N_4O_{11}Cl_2Cu$	$C_{14}H_{18}N_4O_{12}Cl_2Cu$
fw	474.68	568.80
cryst syst	monoclinic	orthorhombic
space group	$P2_1/c$ (No. 14)	*Pbca* (No. 61)
a, Å	10.678 (2)	20.041 (9)
b, Å	16.373 (4)	10.056 (3)
c, Å	9.969 (2)	21.447 (7)
β, deg	106.51 (1)	
V, Å^3	1671.0 (5)	4322 (3)
Z	4	8
D_{calc}, g cm^{-3}	1.89	1.75
μ, cm^{-1}	16.9	13.3
transm coeff	0.93–1.00	0.76–1.00
no. of obsd data ($I > 3\sigma(I)$)	1535	1724
$R(F_o)^a$	0.068	0.058
$R_w(F_o)^b$	0.084	0.074

$^a R = \sum||F_o| - |F_c||/\sum|F_o|$. $^b R_w = [\sum w(|F_o| - |F_c|)^2/\sum w(F_o)^2]^{1/2}$.

entation of the π-system of pyrazine relative to the copper(II) ion coordination plane is important in the propagation of magnetic exchange interaction.

The related nitrogen heterocycles 2,2′-bipyrimidine (bpm), which is well-known to facilitate antiferromagnetic interactions between transition metal ions,[4,6,10,13,14] and 2,3-bis(2-pyridyl)-pyrazine (dpp) can serve as bis-bidentate bridging ligands, resulting in more tightly bound metal centers. Bis(2-pyridyl)pyrazine separates the metal ions more effectively, easing the steric crowding which can occur with bridging bpm ligands,[18] yet still allows strong magnetic and electronic interaction between metal centers.[19] In this paper we report the preparation of two polymeric copper complexes in which, similar to the case of the pyrazine-bridged polymers, the molecular distances have been maintained, even though the "molecules" have been covalently connected to form an infinite linear polymer.

Experimental Section

Preparation of $Cu(ClO_4)_2$. A 0.45 M solution of $Cu(ClO_4)_2$ was prepared by dropwise addition of perchloric acid to a suspension of 10.0 g of dibasic cupric carbonate in 50 mL of water, until the solution became clear. The solution was then diluted with additional water to a volume of 100 mL.

Preparation of $[Cu(bpm)(H_2O)_2]_x(ClO_4)_{2x}\cdot xH_2O$ (1). Addition of the $Cu(ClO_4)_2$ stock solution (5.0 mL) to bpm (0.178 g, 1.13 mmol) dissolved in a minimal amount of water resulted in a blue solution. Slow evaporation of this solution resulted in blue crystals of **1**.

Caution! Perchlorate salts of metal complexes with organic ligands are potentially explosive; all necessary precautions should be taken.[20]

Preparation of $[Cu(dpp)(H_2O)_2]_x(ClO_4)_{2x}\cdot 2xH_2O$ (2). Addition of the $Cu(ClO_4)_2$ stock solution (5.0 mL) to dpp (0.265 g, 1.13 mmol) dissolved in a minimal amount of ethanol resulted in a green solution. Slow evaporation of this solution yielded green crystals of **2**.

X-ray Crystallographic Analysis. Relevant crystallographic data are given in Table I. Intensity data for both compounds were measured at ambient temperature (294 ± 1 K) using $\omega/2\theta$ scans ($2\theta_{max} = 45.0°$) on a Nicolet R3mV diffractometer with graphite-monochromated MoKα radiation ($\lambda = 0.71073$ Å). Empirical absorption corrections and Lorentz and polarization corrections were applied to the data; no correction for extinction was made. The structures were solved by direct methods and refined by full-matrix, least-squares techniques. All non-hydrogen atoms of the cations were refined with anisotropic thermal parameters. The perchlorate anions of both structures were disordered; satisfactory models of each were refined with anisotropic thermal parameters for all atoms other than partial-occupancy oxygen atoms, which were refined with isotropic thermal parameters. Hydrogen atoms were included in the structure factor calculation at optimized positions. Data reduction and correction, structure solution and refinement, and the calculation of derived results were performed with the SHELXTL-PLUS[21] package of programs. Neutral-atom scattering factors were those of Cromer and Waber,[22] and the real and imaginary anomalous dispersion corrections were those of Cromer.[23]

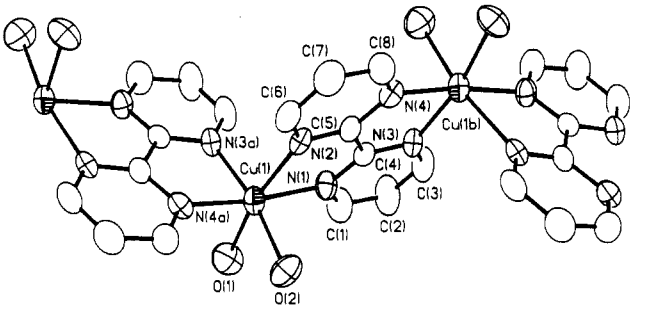

Figure 1. Thermal ellipsoid plot (50% probability) of the Cu(bpm)$(H_2O)_2$ fragment (**1**). Atoms labeled with "a" are related to unlettered atoms by the symmetry operation x, $^1/_2 - y$, $-^1/_2 + z$; atoms labeled with "b" are related by the symmetry operation x, $^1/_2 - y$, $^1/_2 + z$.

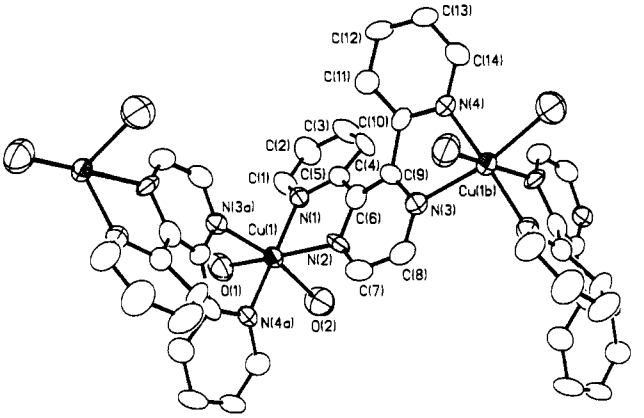

Figure 2. Thermal ellipsoid plot (50% probability) of the Cu(dpp)$(H_2O)_2$ fragment (**2**). Atoms labeled with "a" are related to unlettered atoms by the symmetry operation $-x$, $-^1/_2 + y$, $^1/_2 - z$; atoms labeled with "b" are related by the symmetry operation $-x$, $^1/_2 + y$, $^1/_2 - z$.

Results and Discussion

Thermal ellipsoid plots of the polymeric cation chains for **1** and **2** are shown in Figures 1 and 2, respectively. Atomic coordinates and equivalent isotropic thermal parameters for both compounds are given in Table II.

The two structures are quite similar, with two bis-bidentate ligands, bound in a cis configuration, bridging metal centers which are related by glide-plane symmetry for **1** and screw-axis symmetry for **2**. In each case, the other two sites of a distorted octahedral coordination sphere are occupied by aquo ligands.

The Cu–N distances in the bpm polymer, **1** (mean = 2.1 (1) Å; range = 2.023 (7)–2.319 (8) Å), and the dpp polymer, **2** (mean = 2.09 (9) Å; range = 2.005 (7)–2.176 (8) Å), are quite similar to those observed for $Cu(bpy)_3^{2+}$ [24] (mean = 2.1 (2) Å; range = 2.026 (5)–2.450 (7) Å). Thus, the molecular distances have been maintained even though the "molecules" have been covalently connected to form infinite, linear polymers.

Although the two polymers have a similar stereochemical arrangement of ligands about the six-coordinate copper(II) centers, the pseudo-Jahn–Teller distortion observed for these two d^9 systems is surprisingly different. In **1**, there is one long axis (N(2)/O(1)) with an average bond length of 2.316 (4) Å, while the average bond length in the plane perpendicular is 2.03 (2) Å. In **2**, the bonds along one axis (N(1)/N(4a)) are shortened to an average of 2.008 (4) Å, while the average bond length in the plane per-

(18) Brewer, K. J.; Murphy, W. R.; Petersen, J. D. *Inorg. Chem.* **1987**, *26*, 3376.
(19) Gafney, H. D.; Strekas, T. C.; Baker, A. P.; Braunstein, C. H. *Inorg. Chem.* **1984**, *23*, 857.
(20) Raymond, K. N. *Chem. Eng. News* **1983**, *61* (Dec 5), 4. Wolsey, W. C. *J. Chem. Educ.* **1973**, *50*, A335; *Chem. Eng. News* **1963**, *41* (July 8), 47.
(21) Sheldrick, G. M. *SHELXTL-PLUS, Crystallographic Computing System*; Nicolet Instruments Division: Madison, WI, 1986.
(22) Cromer, D. T.; Waber, J. T. *International Tables for X-ray Crystallography*; Kynoch Press: Birmingham, England, 1974; Vol. IV, Table 2.2B.
(23) Cromer, D. T. *International Tables for X-ray Crystallography*; Kynoch Press: Birmingham, England, 1974; Vol. IV, Table 2.2B.
(24) Anderson, O. P. *J. Chem. Soc., Dalton Trans.* **1972**, 2597.

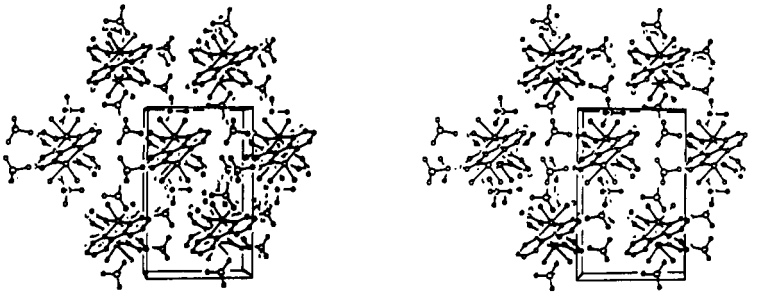

Figure 3. Stereoview of the crystal packing for **1**, viewed down the crystallographic *c* axis, parallel to the polymer chains.

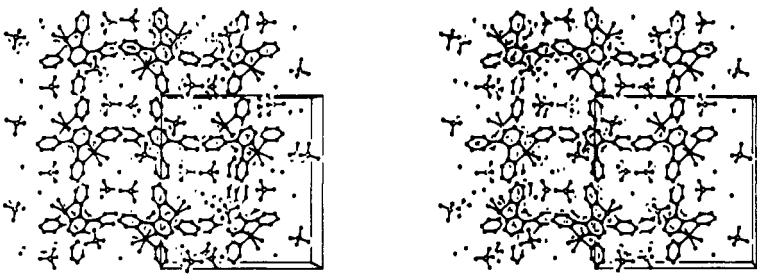

Figure 4. Stereoview of the crystal packing for **2**, viewed down the crystallographic *b* axis, parallel to the polymer chains.

Table II. Selected Atomic Coordinates and Equivalent Isotropic Thermal Parameters

	x/a	*y/b*	*z/c*	U_{eq},[a] Å^2
		Compound **1**		
Cu(1)	0.7428 (1)	0.1717 (1)	0.0752 (1)	0.038 (1)
O(1)	0.8835 (7)	0.0738 (5)	0.0336 (8)	0.063 (3)
O(2)	0.6433 (6)	0.0763 (5)	0.1218 (7)	0.053 (3)
N(1)	0.8478 (7)	0.1845 (5)	0.2787 (8)	0.039 (3)
N(2)	0.6152 (7)	0.2622 (5)	0.1583 (7)	0.034 (3)
N(3)	0.8468 (7)	0.2451 (5)	0.4957 (7)	0.038 (3)
N(4)	0.6276 (7)	0.3248 (5)	0.3753 (8)	0.037 (3)
C(1)	0.958 (1)	0.1466 (8)	0.342 (1)	0.059 (5)
C(2)	1.017 (1)	0.1558 (8)	0.483 (1)	0.068 (6)
C(3)	0.9598 (9)	0.2060 (7)	0.558 (1)	0.054 (5)
C(4)	0.7962 (8)	0.2324 (6)	0.3587 (9)	0.032 (4)
C(5)	0.6720 (8)	0.2755 (6)	0.2903 (9)	0.033 (4)
C(6)	0.5030 (9)	0.3016 (7)	0.103 (1)	0.041 (4)
C(7)	0.4507 (9)	0.3530 (7)	0.183 (1)	0.050 (5)
C(8)	0.5149 (9)	0.3629 (7)	0.319 (1)	0.042 (4)
		Compound **2**		
Cu(1)	0.0887 (1)	0.1115 (1)	0.1723 (1)	0.035 (1)
O(1)	0.1285 (4)	−0.0253 (7)	0.1022 (3)	0.063 (3)
O(2)	0.1689 (4)	0.2485 (9)	0.1400 (4)	0.069 (3)
N(1)	0.0229 (4)	0.1933 (7)	0.1133 (3)	0.034 (3)
N(2)	0.0493 (3)	0.2709 (7)	0.2284 (3)	0.035 (3)
N(3)	−0.0263 (4)	0.4506 (7)	0.2930 (3)	0.036 (3)
N(4)	−0.1459 (3)	0.5293 (7)	0.2610 (4)	0.037 (3)
C(1)	0.0224 (5)	0.168 (1)	0.0532 (5)	0.050 (4)
C(2)	−0.0126 (6)	0.240 (1)	0.0100 (5)	0.057 (4)
C(3)	−0.0480 (6)	0.348 (1)	0.0311 (5)	0.055 (4)
C(4)	−0.0469 (5)	0.380 (1)	0.0948 (5)	0.044 (3)
C(5)	−0.0135 (4)	0.2970 (9)	0.1341 (4)	0.037 (3)
C(6)	−0.0061 (5)	0.3238 (9)	0.2019 (4)	0.036 (3)
C(7)	0.0666 (5)	0.310 (1)	0.2840 (5)	0.044 (4)
C(8)	0.0321 (5)	0.411 (1)	0.3155 (4)	0.044 (4)
C(9)	−0.0489 (4)	0.4015 (9)	0.2397 (4)	0.033 (3)
C(10)	−0.1200 (5)	0.4283 (8)	0.2281 (4)	0.032 (3)
C(1)	−0.1606 (5)	0.348 (1)	0.1918 (5)	0.046 (4)
C(12)	−0.2290 (5)	0.377 (1)	0.1886 (5)	0.051 (4)
C(13)	−0.2532 (5)	0.483 (1)	0.2204 (5)	0.051 (4)
C(14)	−0.2129 (5)	0.557 (1)	0.2565 (5)	0.048 (4)

[a] U_{eq} is defined as one-third the trace of the orthogonalized U_{ij} tensor.

pendicular is 2.19 (3) Å. The elongated, tetragonal distortion in **1** is typical of a Cu(II) 3d^9 electronic configuration of $(xz)^2$,-$(yz)^2$,$(xy)^2$,$(z^2)^2$,$(x^2-y^2)^1$. However, the axial compression found in **2** suggests an inverse Jahn–Teller distortion, which is much less common[25] and requires an electronic configuration of $(xz)^2$,$(yz)^2$,$(xy)^2$,$(z^2)^1$,$(x^2-y^2)^2$. Current work involving the Zn(II) analogue is underway to determine whether the distortion observed in **2** is indeed a Jahn–Teller phenomenon or is a result of packing interactions.

Table III. Selected Bond Distances (Å) and Angles (deg)

	1	**2**
Cu(1)–O(1)	2.313 (8)	2.189 (8)
Cu(1)–O(2)	2.016 (7)	2.228 (8)
Cu(1)–N(1)	2.031 (7)	2.005 (7)
Cu(1)–N(2)	2.319 (8)	2.153 (7)
Cu(1)–N(3a)	2.055 (9)	2.176 (8)
Cu(1)–N(4a)	2.023 (7)	2.011 (8)
O(1)–Cu(1)–O(2)	85.2 (3)	84.9 (3)
O(1)–Cu(1)–N(1)	92.8 (3)	93.6 (3)
O(1)–Cu(1)–N(2)	169.7 (3)	170.0 (3)
O(1)–Cu(1)–N(3a)	86.6 (3)	88.7 (3)
O(1)–Cu(1)–N(4a)	95.0 (3)	91.3 (3)
O(2)–Cu(1)–N(1)	91.6 (3)	91.4 (3)
O(2)–Cu(1)–N(2)	90.6 (3)	88.7 (3)
O(2)–Cu(1)–N(3a)	168.8 (3)	168.8 (3)
O(2)–Cu(1)–N(4a)	92.1 (3)	93.7 (3)
N(1)–Cu(1)–N(2)	77.9 (3)	78.8 (3)
N(1)–Cu(1)–N(3a)	96.4 (3)	98.2 (3)
N(1)–Cu(1)–N(4a)	171.6 (3)	173.2 (3)
N(2)–Cu(1)–N(3a)	98.7 (3)	98.7 (3)
N(2)–Cu(1)–N(4a)	94.5 (3)	96.8 (3)
N(3a)–Cu(1)–N(4a)	81.1 (3)	77.2 (3)

Another interesting aspect of these polymers is the crystal packing. Stereoviews of the crystal packing, viewed parallel to the polymer chains, for complexes **1** and **2** are given in Figures 3 and 4, respectively. In **2**, the polymer chains are situated at the four corners of a near-square; van der Waals contacts between pyridyl rings of adjacent polymer chains enclose channels running parallel to the polymer chains. The perchlorate anions and solvent water molecules are held within these channels by weak hydrogen bonding. In **1**, the polymer chains are in similar positions, but due to the decreased steric interaction of adjacent chains, the channels for the anions and solvent molecules are less defined. In either case, it may be possible to exchange the perchlorate anions for polymeric anionic chains, such as polyiodides, to give a parallel polymer chain network.

Attempts to generate mixed-valence complexes by partially reducing **1** coulometrically, in most solvents, results in polymer

(25) Huheey, J. E. *Inorganic Chemistry*; Harper & Row: New York, 1983; pp 400–401, Table 9.12 (and references, therein).

breakdown to give smaller oligomer units. In fact, if water is added to an evaporated ethanol/water solution containing polymer crystals and mother liquor, the polymer crystals redissolve. Upon reevaporation, the first material to crystallize is the dimeric complex $\{[Cu(bpm)(H_2O)_2]_2(bpm)\}(ClO_4)_4$ (**3**), as confirmed by X-ray crystallography.[25] As the mother liquor continues to evaporate, the dimeric crystals dissolve and polymer crystals reform. Presumably, this occurs because of the Cu:bpm ratio according to the following: (1) The first compound to form is the kinetically-favored, dimeric complex **3**, with a Cu:bpm ratio of 2:3. (2) As this cation crystallizes (with ClO_4^-), the Cu:bpm ratio in solution increases, favoring the formation of larger oligomers. (3) As larger oligomers are formed, the thermodynamically-favored polymer (Cu:bpm ratio of 1:1) is formed by dissolution of the dimeric crystals to add to the chain length in solution. (4) Continued evaporation results in crystallization of the infinite-chain polymer complex.

Isolation of a single-crystal dimeric Cu(I) species, $\{[Cu(bpm)]_2(bpm)\}(BPh_4)_2$,[26] suggests that a mixed-valence system will be capable of forming ordered crystalline materials. Mixed-metal systems, such as Cu(II)/Fe(II), are also being investigated.

Acknowledgment. J.D.P. thanks the Office of Basic Energy Sciences, U.S. Department of Energy, for partial support of this work.

Supplementary Material Available: For **1** and **2**, complete listings of atomic coordinates, distances and angles, anisotropic thermal parameters, and crystallographic data (10 pages); tables of observed and calculated structure factors (18 pages). Ordering information is given on any current masthead page.

(26) Morgan, L. W.; Pennington, W. T.; Petersen, J. D. Work in progress.

Contribution from the Departments of Chemistry, Indian Institute of Technology, Powai, Bombay 400076, India, and University of Delaware, Newark, Delaware 19711

Synthesis and Characterization of the New Mixed-Metal Cluster Complexes $[Fe_2M(\mu_3\text{-}E)_2(CO)_{10}]$ (M = W, E = Se, Te; M = Mo, E = Se). Crystal Structure of $[Fe_2W(\mu_3\text{-}Te)_2(CO)_{10}]$

Pradeep Mathur,*,† Debojit Chakrabarty,† Md. Munkir Hossain,† Raad S. Rashid,† V. Rugmini,† and Arnold L. Rheingold*,‡

Received August 15, 1991

Intense interest in transition-metal clusters continues because they represent possible conceptual bridges between homogeneous and heterogeneous catalysts and also because they represent synthetic challenges. A further challenge is represented by attempts to prepare mixed-metal clusters.

The oxidative addition of the E–E linkage of $(\mu\text{-}E_2)Fe_2(CO)_6$ (E = S, Se, Te) to various low-valent, transition-metal species has yielded many mixed-metal complexes bridged by chalcogen atoms.[1] Seyferth and co-workers developed this method for the addition of various mononuclear species, such as $Ni(Ph_2PCH_2CH_2PPh_2)$, $Pd(PPh_3)_2$, $Pt(PPh_3)_2$, CpCo, and Me_2Sn, across the S–S bond of $(\mu\text{-}S_2)Fe_2(CO)_6$.[2] Polynuclear metal carbonyl species, "$Ru_3(CO)_{11}$"[3] and "$Os_3(CO)_{11}$",[4] can also add across the Te–Te bond of $(\mu\text{-}Te_2)Fe_2(CO)_6$. In general, the aggregation of metal atoms frequently occurs in one of the two ways shown by eqs 1 and 2.

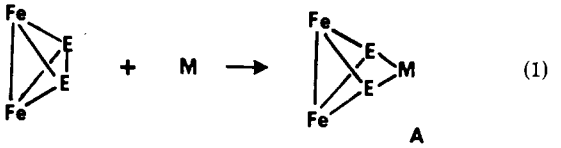

(1)

A

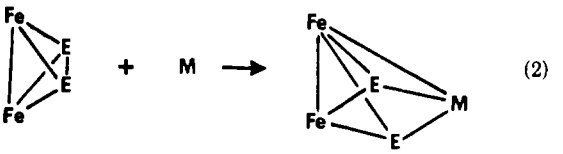

(2)

B

By the first route, a metal-containing group inserts into the E–E bond and no metal–metal bonds are formed. In the second route, insertion of a metal-containing group into the E–E bond is accompanied by the formation of an Fe–M bond to form a square-pyramidal Fe_2E_2M core, in which the M atom occupies a basal site. Species such as B could be formed via A. For instance, $(CO)_6Fe_2(\mu_3\text{-}Te)_2Fe(CO)_3PPh_3$ (structure A) readily undergoes decarbonylation to form $Fe_3(CO)_8(PPh_3)(\mu_3\text{-}Te)_2$ (structure B).[5] A third possibility (structure C) is the formation

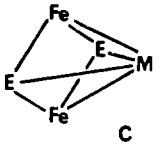

C

of an Fe_2ME_2 square pyramid, in which M occupies the apex. Formation of C would involve insertion of M into the E–E bond, accompanied by cleavage of the Fe–Fe bond and formation of two Fe–M bonds. Examples of compounds with type C structures are far fewer than those exhibiting type A or B structures. In $(C_5H_4COOMe)CoFe_2(CO)_6(\mu_3\text{-}S)_2$[6] and $Fe_2W(CO)_9(PMe_2Ph)(\mu_3\text{-}S)_2$,[7] crystallographic analyses have revealed that the metal heteroatom occupies the apical site of a square pyramid. Rauchfuss has reported that $(C_5H_5)RhFe_2(CO)_6(\mu_3\text{-}Te)_2$ exists in two isomeric forms, one having a B-type structure and the other a C-type structure.[1c]

Table I. Crsytallographic Data for $Fe_2WTe_2(CO)_{10}$

chem formula $C_{10}Fe_2O_{10}Te_2W$	fw 830.8
a = 7.010 (3) Å	space group $P\bar{1}$
b = 9.591 (2) Å	T = 25 °C
c = 13.733 (5) Å	λ = 0.710 73 Å
α = 80.79 (2)°	ρ_{calcd} = 3.06 g cm^{-3}
β = 82.74 (3)°	μ = 116.9 cm^{-1}
γ = 84.73 (3)°	$R(F)^a$ = 3.99%
V = 901.7 (6) Å^3	$R_w(F)^b$ = 4.39%
Z = 2	

$^a R(F) = \sum|F_o - F_c|/\sum F_o$. $^b R_w(F) = \sum(|F_o - F_c|w^{1/2})/\sum(F_o w^{1/2})$.

† Indian Institute of Technology.
‡ University of Delaware.

(1) (a) Vahrenkamp, H.; Wucherer, E. J. *Angew. Chem., Int. Ed. Engl.* **1981**, *93*, 715. (b) Lesch, D. A.; Rauchfuss, T. B. *Inorg. Chem.* **1983**, *22*, 1854. (c) Day, V. W.; Lesch, D. A.; Rauchfuss, T. B. *J. Am. Chem. Soc.* **1982**, *104*, 1290. (d) Mathur, P.; Mavunkal, I. J.; Rugmini, V.; Mahon, M. F. *Inorg. Chem.* **1990**, *29*, 4838. (e) Chakrabarty, D.; Hossain, Md. M.; Mathur, P. *J. Organomet. Chem.* **1991**, *401*, 167.
(2) (a) Seyferth, D.; Henderson, R. S.; Gallagher, M. K. *J. Organomet. Chem.* **1980**, *193*, C75. (b) Seyferth, D.; Henderson, R. S.; Song, L.-C. *Organometallics* **1982**, *1*, 125.
(3) Mathur, P.; Mavunkal, I. J.; Rheingold, A. L. *J. Chem. Soc., Chem. Commun.* **1989**, 382.
(4) Mathur, P.; Mavunkal, I. J.; Rugmini, V. *Inorg. Chem.* **1989**, *28*, 3616.
(5) Lesch, D. A.; Rauchfuss, T. B. *Organometallics* **1982**, *1*, 499.
(6) Wakatsuki, Y.; Yamazaki, H.; Cheng, G. *J. Organomet. Chem.* **1988**, *347*, 151.
(7) Adams, R. D., Babin, J. E.; Wang, J.-G.; Wu, W. *Inorg. Chem.* **1989**, *28*, 703.

0020-1669/92/1331-1106$03.00/0